International Journal of Computing and Digital Systems
ISSN (2210-142X)
Int. J. Com. Dig. Sys. 9, No.1 (Jan-2020)

http://dx.doi.org/10.12785/ijcds/090108

Harmonic Analysis of Photovoltaic Generation in Distribution Network and Design of Adaptive Filter

Lue Xiong [1], Mutasim Nour [1] and Eyad Radwan[2]

[1] *School of Engineering and Physical Sciences Heriot-Watt University Dubai, Dubai, UAE*
[2] *Electrical Engineering, Applied Science University, Amman, Jordan*

Received 30 Jul. 2019, Revised 21 Oct. 2019, Accepted 18 Dec. 2019, Published 01 Jan. 2020

Abstract: The aim of this paper is to investigate the effect of increased penetration level of Photovoltaic (PV) generation on the distribution network. Harmonic distortion is the main factor studied in this paper and a typical three-bus distribution network is built in MATLAB/Simulink to understand the harmonics problem. The obtained results show that current harmonics are more susceptible to fluctuate compared to voltage harmonics. Based on existing IEEE harmonic standards, total demand distortion of current (TDDi) is evaluated to estimate maximum PV penetration level at Point of Common Coupling (PCC), and the maximum acceptable TDDi at each bus differs according to specific loading and short-circuit levels. Meanwhile, total harmonic distortion of current (THDi) at inverter outputs represents inverter performance. Instead of assessing at standard test conditions (STC), the impact of irradiance variations is studied. Low irradiance results in an increased THDi of the inverter whilst doesn't explicitly affect TDDi at PCC. A simple and low-cost solution is proposed to dynamically vary the settings of inverter's filter elements against irradiance, and harmonic distortion at low irradiance of the inverter is successfully mitigated.

Keywords: total harmonic distortion, total demand distortion, irradiance, PV penetration level, power system

1. INTRODUCTION

Photovoltaic (PV) generation is one widely applied form of Renewable Energy Generation (REG), which turns universally available solar energy into electricity through photovoltaic effect [1]. The whole generation process is independent of fossil fuels, and the massive usage of PV technologies is in line with sustainable goals and renewable targets proposed worldwide. Moreover, recent price drops in solar panels since 2010 have boosted PV installations globally and the cumulative installed capacity of PV panels worldwide has reached 385GW in 2017 [2]. Supported by various incentive plans and more large-scale development contracts, the overall PV industry is expected to follow the current exponential trend of development in the coming ten years.

Unlike fossil fuels, the intermittent and non-dispatchable nature of REG pose new threats to power systems, and potential impacts include voltage fluctuations, harmonics, reverse power flows and malfunction of protection devices [3]. Meanwhile, the PV generation can be either connected to transmission or distribution network, and the severity of corresponding problems also varies. For instance, from statistics in Greek power system, 97.8% of PV system are connected at the voltage levels of 20kV and 0.4kV, and the lack of control schemes like active power curtailment indicates PV generation is more problematic in the distribution network [4].

Inverter which transforms energy forms from DC to AC is a basic element in PV system. However, the conversion process can inject undesired harmonics at lower order into power system [5]. Excessive harmonic voltage and current induce extra losses like core losses in transformers and generators, as well as increase transmission losses in conductors, which further cause overheating and affect lifecycles of power equipment and potentially result in maloperation of protective devices [6]. Since the inverter is the main source of harmonics, most inverter datasheets specify the maximum distortion limit at rated output conditions. For instance, SUN2000-8/12KTL manufactured by HUAWEI sets the maximum distortion limit to 3% at STC [7]. Obviously, solar inverters cannot always work under rated conditions. Typical Meteorological Year (TMY) data in Dubai is used for illustration, which presents best-fit weather data for the past ten years (between 2007-2014). The TMY data sources come from Photovoltaic Geographical Information System [8], which includes 8760 hourly samples in total. Excluding samples without solar

Email Address: lx9@hw.ac.uk, mutasim.nour@hw.ac.uk, e_redwan@asu.edu.jo

generation, the probability occurrence of solar irradiance is presented in Fig.1, which indicates that solar inverter doesn't work under STC for most occasions. However, existing grid codes and testing procedures about harmonic injections from inverters are mostly based on rated outputs under STC. Hence, harmonic levels under low irradiance should also be considered in the design.

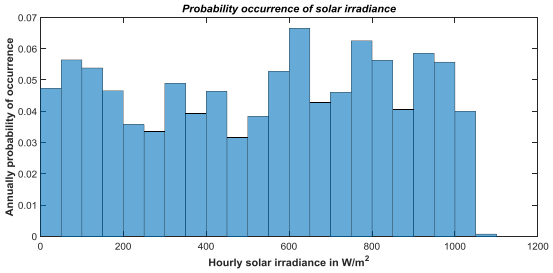

Figure 1. Probability occurrence of solar irradiance (TMY data in Dubai)

The commonly used indicator to reflect the distortion levels is Total Harmonic Distortion (THD) which is the ratio of the rms magnitude of the harmonics (excluding fundamental) to the fundamental rms value [9]. THD expression for current is given by:

$$\mathrm{THD}_i = \sqrt{\sum_{n=2}^{\infty} I_n^2} \Big/ I_1 \qquad (1)$$

Where I_1 is the rms fundamental current, I_n is the rms value of current at n^{th} harmonics. Same formula applies to THD expression for voltage.

Various standards such as IEEE 919, IEEE 519-2014, IEC 61000, IEC 61727 and EN 50160 are proposed by industry to regulate harmonic injections within proper levels. Instead of using fixed harmonic distortion limits, IEEE standards set harmonic constraints based on voltage levels and the ratio of maximum short-circuit current (I_{sc}) to maximum demand current (I_L). Specifically, current distortion limits are presented in Table I, which vary under different I_{sc}/I_L [10].

TABLE I. MAXIMUM HARMONIC CURRENT DISTORTION IN PERCENT OF IL INDIVIDUAL HARMONIC ORDER (ODD HARMONICS)

I_{sc}/I_L	<11	11≤h<17	17≤h<23	23≤h<35	23≤h≤50	TDD
<20	4.0	2.0	1.5	0.6	0.3	5.0
20<50	7.0	3.5	2.5	1.0	0.5	8.0
50<100	10.0	4.5	4.0	1.5	0.7	12.0
100<1000	12.0	5.5	5.0	2.0	1.0	15.0
>1000	15.0	7.0	6.0	2.5	1.4	20.0

The application of I_{sc}/I_L ratio is a good representation of relative importance of the studied target on power system in terms of harmonic injection [11]. Specifically, a higher I_{sc}/I_L value indicates that demand current is insignificant compared to the network size, thus a high distortion limit is allowed since this impact is minimal. As described in (2), Total Demand Distortion (TDD) mentioned in Table I is the ratio of the square root of the total squared harmonic current components to the maximum load current.

$$\mathrm{TDD}_i = \sqrt{\sum_{n=2}^{\infty} I_n^2} \Big/ I_L \qquad (2)$$

Where I_n is the rms value of current at n^{th} harmonics, and I_L is the maximum load current.

Several researchers have studied harmonic scenarios against irradiance variations either using computational software tools or via experimental testing. In [12], PQ analyzer is used in the 1.22MW rooftop PV system in University of Queensland for harmonic measurements. The obtained results show that THD_v is within IEEE standards during the day and reaches to maximum at peak solar generation (1.4%). On the other hand, THD_i is inversely proportional with solar irradiance since the fundamental current is less during early morning and late afternoon. A field test of a 20kW PV system in Greece is implemented in [13], and harmonic distortions are poor under sunrise and sunset hours, whilst 3rd harmonic components are relatively significant. Similarly, based on detailed inverter models, authors in [14] found that THD_i increases at lower irradiance compared to Standard Test Condition (STC) of 1000 W/m^2 whilst THD_v maintains the same. The impact of solar irradiance on THD_v and THD_i is also studied in [15]. Results show that THD_i is more vulnerable to irradiance variations and IEEE limits are breached under low irradiance of 161 W/m^2. However, differences between THD_i and TDD_i haven't been identified and addressed in the abovementioned papers.

Two of the commonly used solutions to mitigate harmonic problems are adding extra filters and modifying inverter controllers. In [16], the combination of a notch filter and a high-pass filter is added in parallel with existing capacitors to reduce both THD_v and THD_i. Likewise, a DSP controller-based shunt active filter is proposed in [17]. The controller reduces harmonics and compensates reactive power. In [18], an LCL-based filter of the solar inverter is modified using harmonic compensators, which selectively decreases the 3rd, 5th and 7th harmonics. A hybrid proportional-resonant (PR) controller and repetitive controller is designed in [19] to address THD_i issues with specially tuned parameters. However, PR controller performs well only for single-phase inverter, which limits its application range. The idea of generating mirror harmonics using buck-boost converter to cancel original voltage harmonics is implemented in [20], but the function of this algorithm in mitigating current distortion is not discussed. A PV integrated shunt active power filter using adaptive linear neuron algorithm is proposed in [21]. Although the authors claimed that the performance of the algorithm is good over a wide range of solar irradiance, the implementation of such algorithm requires a powerful DSP which may add to the complexity and cost of the

inverter system. The authors in [22] presented an adaptive harmonic compensation algorithm in residential distribution grid for roof top PV system based on the measurement of the point of common coupling voltage harmonic. The proposed technique requires individual compensation of the measured harmonics using model predictive current controller. However, the effectiveness of the algorithm is not tested for solar irradiance variation, especially at low values when the THD is expected to increase. Instead of adding extra complexities into inverter designs, a simple and cost-saving method is proposed in this paper. Furthermore, as mentioned in [19], harmonic levels at low irradiance conditions may break grid requirements but have not been explicitly covered in present standards. Hence, different operating conditions under irradiance variations are also studied and tested.

To quantify the maximum PV capacity that the distribution network can sustain, the PV penetration factor (PVPF) is introduced as the ratio of the aggregated PV capacity in specified area to the rating of distribution transformer which provides local services [23]. Its formula is given in (3). The maximum PVPF is limited by either voltage or current harmonic constraints mentioned in IEEE std 519-2014.

$$PVPF = (C_{PV} / S_{TF}) \times 100\% \quad (3)$$

Where C_{PV} is the aggregated PV capacity within specified area (kWh); S_{TF} is rating of distribution transformer (kVA).

The aim of this paper is to investigate maximum PV penetration level and its effects on the acceptable harmonic standards. Matlab/Simulink is used to simulate the harmonic problem caused by PV penetration within a typical distribution network, incorporating scenarios like irradiance variations. Also, a simple and low-cost measure is proposed and implemented to mitigate the harmonic problem.

2. METHODOLOGY

A. PV penetration in three-bus distribution network

In Fig.2, a typical 25kV/60Hz distribution network in North American is used, and three buses are connected radially [24]. The whole system is implemented in Matlab/Simulink.

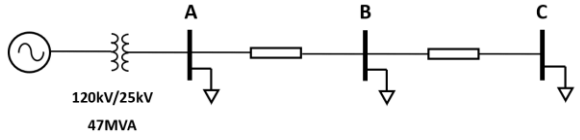

Figure 2. Single line diagram of three-bus distribution network

Load information is presented in Table II, which is modified from the original network.

TABLE II. LOAD DETAILS FOR THREE-BUS NETWORK

Bus	Active P	Reactive Q	Power Factor
A	30MW	2MVAr	0.99
B	2MW	0	1
C	250kW	0	1

With reference to [24], a 250kW PV system is designed and its generic diagram is shown in Fig.3. The key components are introduced separately.

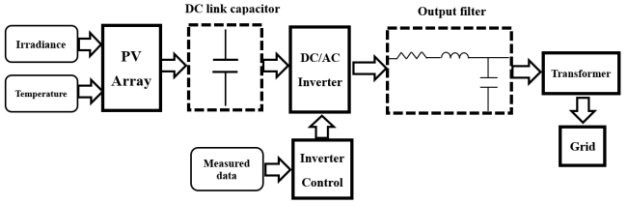

Figure 3. Single line diagram of three-bus distribution network

To obtain PV capacity of 250kW, the industry-verified PV panel (SunPower SPR-415E-WHT-D) is selected with 415W as DC capacity. 88 panels are connected in parallel with 7 panels connected in series. The three-level based IGBT bridge circuit is implemented for DC/AC conversion. The converter is pulse width modulated (PWM), which is used in the inverter control block.

DC link capacitor is required to compensate 120 Hz power ripple on the DC bus caused by the AC load side of the inverter [25]. The required capacitance to buffer the ripple is based on the output power during 1/8th fundamental cycle, which is given in [25]:

$$P_{ac} = \Delta E/(T/8) = (1/2)\left[CV^2 - C(V-\Delta V)^2\right] \times 8 f_{ac} \quad (4)$$
$$C_{link} = (P_{ac}/4 f_{ac}) \times \left[1/(2V\Delta V - \Delta V^2)\right] = (P_{ac}/4 f_{ac}) \times (1/2V\Delta V)$$

Where, P_{ac} is rated output power in kW from AC side - 250kW, f_{ac} is 60Hz, V is DC voltage decided by PV array -480V for 7 panels in series, ΔV is the specified maximum voltage ripple, also power ripple.

In (4), ΔV^2 is regarded as minimal which can be neglected. Assume power ripple (ΔV) of 40V is acceptable, so the value of required capacitance is calculated as:

$$C_{link} = \left[250 \times 10^3/(4 \times 60)\right] \times (1/2 \times 480 \times 40) = 0.0271F \quad (5)$$

The three-level based IGBT bridge circuit is implemented for DC/AC conversion. Maximum Power Point Tracking (MPPT) block, Phase-locked loop (PLL) unit, PWM generator, and the current/voltage regulator circuit are principal components inside the inverter control block. The MPPT algorithm is based on Perturb and Observe (P&O), which periodically perturbs output voltage to obtain maximum power [26]. PLL is for

synchronization of phase angles. PWM generates pulses to control IGBT switches. The carrier frequency is selected as 33 times fundamental frequency, which is 1980Hz. Finally, the design of regulator circuit is like the structure of current controlled voltage source inverter (VSI) proposed in [27] and [28], which transforms three-phase signals into dq0 frames to generate reference signals. Default settings in [24] are used during simulation.

The output filter is mainly designed for smoothing out harmonics. A series RL choke circuit and a C-filter in parallel. The RL choke, also known as line reactor, is designed to attenuate harmonics and protect equipment against transient overshoots [29]. The inductance dominants in the choke circuit, and (6) shows calculation process [30].

$$L_{choke} = k \times (1/2\pi f_{ac}) \times \left(V_{L-L}/\sqrt{3}\, I_{rms}\right) = kV_{L-L}^2/2\pi f_{ac} P_{ac} = \left(0.15 \times 250^2\right)/\left(2\pi \times 60 \times 250 \times 10^3\right) = 9.95 \times 10^{-5} H \quad (6)$$

Where V_{L-L} is the line voltage at the inverter output (250V) obtained from DC link voltage, I_{rms} is rms current flowing through choke inductor, k value is 0.15 by default.

The C-type filter is used for reducing harmonics and improving reactive power. A small capacitor is designed with its rated reactive power is 10% of rated PV output.

B. Adaptive inverter filter settings

Instead of altering inverter control logic or adding a separate filter, a simple method which changes the settings of passive filter elements is presented. As shown in (4) and (6), parameters like f_{ac}, V and V_{L-L} have less fluctuations because of grid connection and inverter control logics and hence can be regarded as constants. Since active power P_{ac} is directly proportional to irradiance, the relationship between passive elements and irradiance is given in (7) and (8).

$$C_{link} = \left(P_{ac}/4 f_{ac}\right) \times \left(1/2V\Delta V\right) \propto P_{ac} \propto I_{irradiance} \quad (7)$$

$$L_{choke} = kV_{L-L}^2/2\pi f_{ac} P_{ac} \propto 1/P_{ac} \propto I_{irradiance} \quad (8)$$

Where $I_{irradiance}$ is the irradiance level in W/m^2.

The best-fit filter parameters under different irradiance levels should not be constants at rated outputs. Table III lists the optimal filter parameters under different irradiance levels with a gap of 200W/m^2. The feasibility of the proposed adaptive settings is studied through simulation in the following sections.

TABLE III. CALCULATED FILTER PARAMETERS FOR DIFFERENT IRRADIANCE

Irradiance (W/m^2)	1000	800	600	400	200
C_link (F)	0.0543	0.04344	0.03258	0.02172	0.01086
L_choke (H)	9.95E-05	1.24E-04	1.66E-04	2.49E-04	4.98E-04

3. SIMULATING HARMONIC PROBLEM IN THREE-BUS POWER SYSTEM

In the three-bus distribution network model in Fig.2, the I_{sc}/I_L of each bus is evaluated. I_L is measured as steady-state current flow, whilst I_{sc} is obtained by applying a balanced three-phase fault on each bus. Calculated results are presented in Table IV.

TABLE IV. I_{SC}/I_L RATIO IN THREE-BUS MODEL

Bus	Normal operation		Three phase faults		Isc/IL
	Max. load	Max. load current (I_L)	Fault level	Max. fault current (Isc)	
A	30MW&2MVAr	750A	268MVA	6196A	8.3
B	2MW	52A	77MVA	1783A	34.3
C	250kW	5.7A	55MVA	1264A	222

With reference to IEEE std. 519-1992, allowable voltage and current harmonics (expressed as THDv and TDD_i) for each bus are obtained, with results shown in Table V. Bus C at the end of radial network has highest TDDi of 15%.

TABLE V. HARMONIC LIMITS FOR EACH BUS

Bus	A	B	C
Isc/IL	8.3	34.3	222
Max. TDD_i	5%	8%	15%
Max. THD_v	5%	5%	5%

A. Base case for 250kW at bus C

Based on Fig.1 and Fig.2, the 250-kW PV system is initially connected to bus C, so bus C is the PCC between PV and load. PVPF for this case is evaluated as:

$$PVPF = \left(C_{PV}/S_{TF}\right) \times 100\% = 250kW/47MVA \times 100\% = 0.53\% \quad (9)$$

THD_v and THD_i for each bus under different irradiance levels are measured and presented in Table VI and Table VII. The obtained results show that the THD_v at all buses are negligible under this level of PV penetration. Meanwhile, without any voltage compensation devices, the THD_i harmonic level decreases from bus C to bus A at the source.

TABLE VI. THD_V AT EACH BUS FOR PV AT BUS C

Irrdiance level (W/m^2)	BusA	BusB	BusC
1000	0.01%	0.07%	0.11%
800	0.01%	0.07%	0.10%
600	0.01%	0.07%	0.10%
400	0.01%	0.07%	0.11%
200	0.01%	0.07%	0.10%

TABLE VII. THDI AT EACH BUS FOR PV AT BUS C

Irrdiance level (W/m^2)	BusA	BusB	BusC	Bus PV
1000	0.01%	0.18%	37.95%	1.61%
800	0.01%	0.14%	5.33%	1.67%
600	0.01%	0.14%	2.84%	2.20%
400	0%	0.14%	2.03%	3.49%
200	0%	0.13%	1.48%	6.97%

The relationship between THD_i and TDD_i is described in (10). Both THD_i and TDD_i at bus C are evaluated and shown in Table VIII.

$$THD_i \times I_1 = TDD_i \times I_L \quad (10)$$

TABLE VIII. THD_i AND TDD_i AT BUS C

Irrdiance level (W/m^2)	THDi	I_1(A)	I_L(A)	TDDi
1000	37.95%	0.323	5.7	2.15%
800	5.33%	1.885	5.7	1.76%
600	2.84%	3.465	5.7	1.73%
400	2.03%	5.051	5.7	1.80%
200	1.48%	6.644	5.7	1.73%

In Table VIII, THD_i at 1000W/m^2 is extremely high due to low fundamental current I_1. However, according to IEEE std 519-2014, TDD_i is a true reflection for harmonic distortion at PCC. In this case, TDD_i is around 2% under different irradiance, which is within the 15% limit specified in Table V.

B. *Investigating penetration limit*

To identify allowable penetration limits at each bus, a series of simulation is performed for the PV array of different sizes connected individually to each bus. Assumptions include:

- The size of PV array increases from 500kW with a step size of 500kW (equivalent to 1% PVPF for this radial network);
- Harmonic levels are assessed at two irradiance levels: 1000W/m^2 and 200W/m^2, which represent cases of standard irradiance and low irradiance;
- Simulation stops when any of three criteria (THD_v, TDD_i and individual harmonic levels in Table I) reaches the harmonic limit of this bus at any irradiance level (1000W/m^2 or 200W/m^2).

THD_v variations against increasing PV penetration at bus C is shown in Fig. 4. A positive linear relationship is observed between voltage distortion and PV penetration capacity. THD_v under both is well below specified 5% limit.

The variations of TDD_i against increasing PV penetration at bus C is presented in Fig. 5. In comparison, current distortion at PCC is more significant under standard irradiance compared to low irradiance. The maximum allowable PV capacity at bus C is 1,800kW, which accounts for 3.8% of PVPF.

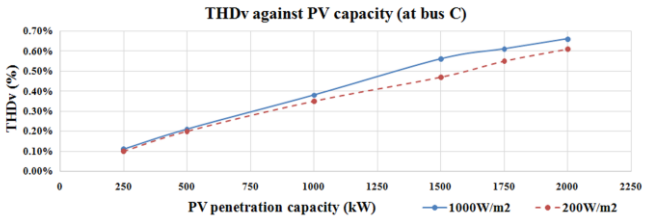

Figure 4. THDv against PV capacity (at bus C)

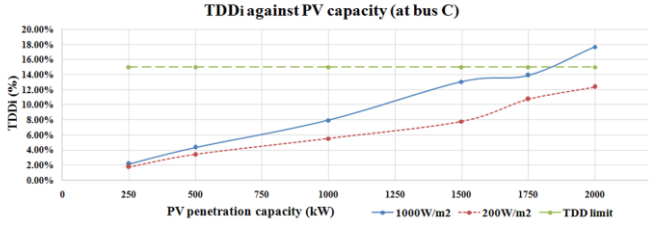

Figure 5. TDDi against PV capacity (at bus C)

Similarly, maximum penetration levels at bus A and bus B are investigated and summarized in Table IX. TDD_i is the dominant factor determining PVPF, and the impact of THD_v is negligible. Results of PVPF show that the bus nearer to the grid can accommodate more PV panels. However, if ratio of PV capacity to local load is considered, the far-end bus can withstand a higher degree of PV penetration. Therefore, case-by-case examination is required for the penetration assessment.

TABLE IX. SUMMARY FOR PV PENETRATION INVESTIGATION

Bus	Max. PVPF	Max. PV level (MW)	Max. load (MW)	PV/load ratio
A	40.4%	19	30	0.6
B	18.1%	9	2	4.5
C	3.8%	1.8	0.25	7.2

C. *Investigating irradiance impact*

To study the impact of irradiance on current distortion at PCC, the same 1,000kW PV array is connected individually to all buses, and TDD_i of all buses under varying irradiance is illustrated in Fig. 6. It is observed that no explicit relationship is identified between TDDi under different irradiance levels. However, in this scenario, all TDDi values reach maximum around standard irradiance of 1000W/m^2, which is also true in previous cases. Therefore, it is recommended to perform current harmonic distortion assessment at PCC under STC, which can represent worst-case scenarios under irradiance fluctuations.

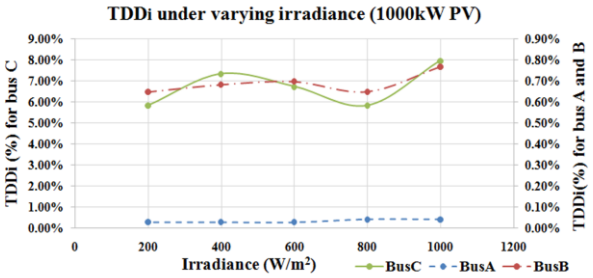

Figure 6. TDDi under varying irradiance with 1000kW PV at each bus

4. ADAPTIVE FILTER SETTING TO MITIGATE HARMONICS

Previous section shows that application of IEEE std 519-2014 at PCC and current distortion is assessed by TDD_i, which describes the interaction between PV and load at PCC. However, to assess the power quality from inverter alone, the THD_i at inverter output should be used. For instance, the last column in Table VII is plotted in Fig. 7 for illustration.

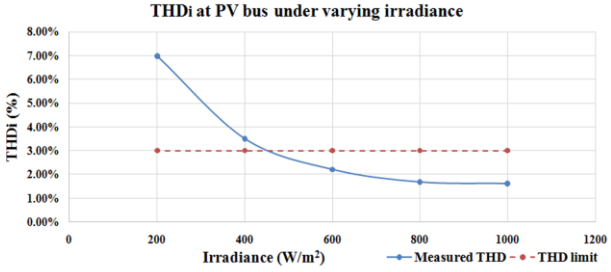

Figure 7. THDi at PV bus under varying irradiance (base case)

Fig. 7 shows that the harmonic level at inverter output is inversely proportional to the irradiance. The 3% distortion limit is breached for irradiance less than 400W/m^2.

As discussed in the methodology part, the optimal filter settings variation under certain irradiance levels is presented in Table III. Using the base case of 250kW PV, simulation is performed to compare cases of nominal settings at STC and adaptive settings. Results are illustrated in Table X and Fig. 8.

TABLE X. THDI AT BUS PV UNDER NOMINAL AND ADAPTIVE CASES

THDi at bus PV under nominal and adaptive cases		
Irradiance (W/m^2)	Nominal	Adaptive
1000	1.61%	1.61%
800	1.67%	1.76%
600	2.20%	1.69%
400	3.49%	1.93%
200	6.97%	1.38%

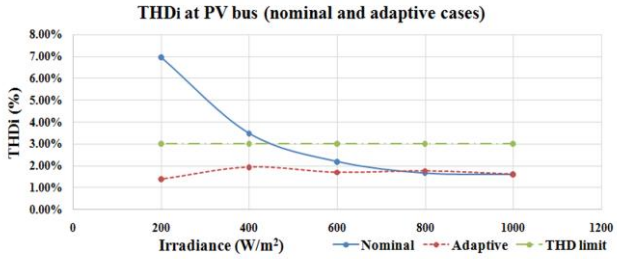

Figure 8. THDi at PV bus (nominal and adaptive cases)

Results show that the proposed adaptive method effectively attenuate harmonics within specified limits, which outperform the fixed nominal settings.

The concept of adaptive settings is like potentiometer, which slides or rotates to proper position to get desired values of passive elements. The control signal can either come from external sensors which measures irradiance or internal lookup table that stores historical irradiance records. In this example, five categories are specified for classifying the input irradiance, and each category corresponds to one group of filter settings. Fig. 9 shows generic control logic.

Although irradiance sensor is more accurate than lookup table in collecting irradiance, it is more costly than lookup table. Meanwhile, the prestored lookup table should be updated to reflect state-of-the-art weather information. High quality weather data is needed for successful implementation. The number of classification groups in Fig. 9 depends on actual application. More group number means more accurate control but increased switch operations which may reduce equipment lifecycles. Overall, the proposed algorithm is cost-effective since only series variable inductor and fixed value capacitor are required.

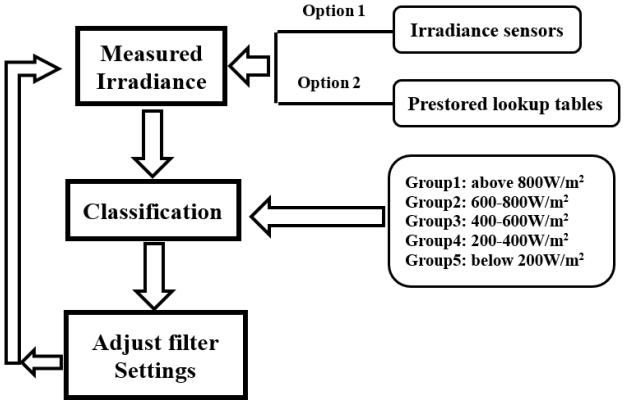

Figure 9. Generic control logic of adaptive inverter settings

5. DISCUSSIONS

Unlike stable voltage profiles, more stochastic factors are imbedded within current profiles, and optimal power balancing is always problematic for network operators. This situation deteriorates under high level PV penetration since distribution network is no longer passive and reverse power flow becomes possible. Three common confusions are clarified in this paper: firstly, current harmonics at PCC should be assessed by TDD_i, which measures harmonics after the combination of PV and load. Therefore, the load of a larger size can generally accommodate more PV penetration. Meanwhile, the harmonic distortion of inverters should be measured by THD_i directly at inverter's output, which is independent of load variations. Secondly, since irradiance intensity can vary from zero to 1000W/m^2 within a day, the impact of irradiance on harmonics should be seriously treated. However, based on available current research, this aspect is not thoroughly investigated. Simulation results show that THD_i of inverter under low irradiance can cause harmonic level above the objective limit of 3% specified in simulation. Therefore, this issue should be addressed and mitigated by inverters manufacturers. In contrast, though the relationship between TDD_i at PCC and irradiance is not explicit, the TDD_i at 1000W/m^2 represents the highest harmonic values compared to all lower irradiance levels in the proposed scenario. Thirdly, the standard current distortion should not be a fixed limit, I_{sc}/I_L ratio should be measured, which indicates the relative importance of load bus on the overall distribution network. All these factors further urge the need to develop an adaptive solution varying filter parameter to mitigate harmonics.

In terms of I_{sc}/I_L ratio, the maximum penetration level at all buses is evaluated and results are presented Table VIII. For the 3-bus test model, more PV generation can be installed at bus A which is nearest to external grid, with a PVPF of 40.4% compared to the transformer size. However, if the size of local load is used as reference, bus C at the bottom of radial network can connect 7 times higher PV capacity without causing harmonic problem. Therefore, maximum PV penetration is recommended to be evaluated based on case-by-case examination where factors like network topology and loading conditions are considered. Furthermore, and as addressed and discussed in [31], under high level of PV penetration the possible synergistic effects among PV array should also be considered, which can be either constructive or destructive in terms of harmonic injections. Larger distribution network models are required to obtain accurate outputs.

To mitigate inverter THD_i problem under varying irradiance, a simple methodology based on adaptive settings of passive elements is proposed and simulated in Simulink. Either accurate irradiance measurements or weather data files is needed to facilitate implementation. Resonance is a common problem shared in power electronics devices, and authors in [32] have identified that filter elements from the inverter are directly related to network resonance. Hence techniques in mitigating resonance should be properly designed in this methodology.

6. CONCLUSIONS

The impact of high PV penetration level on harmonics is studied in this paper. The difference between THD and TDD current distortion is distinguished. Based on the typical distribution network model built in Simulink, results of TDD_i at PCC between PV and load are measured and the PV penetration level positively contributes to the TDD_i increase. Meanwhile, TDD_i limits on each bus are different because of I_{sc}/I_L ratio. More harmonic distortion in percent is allowed when load is insignificant to the grid. The maximum allowable PV capacity at each bus is evaluated, and the obtained results show that the bus nearer to external grid can accommodate more PV penetration. Furthermore, the impact of irradiance variations on TDD_i is minimal, and the TDD_i under standard irradiance of 1000W/m^2 can represent the worst scenario. However, low irradiance affects THD_i at inverter output, which should be mitigated by improving the inverter design. A simple and cost-effective solution is proposed and tested, through adaptive adjustment of passive filter elements with respect to irradiance levels. Reduced harmonics are observed from simulation results. Theoretical analysis and software simulation are principal methodologies applied in this paper, and practical experiments are to be implemented in the next stage.

ACKNOWLEDGMENT

We would like to offer special thanks to Heriot-Watt University Dubai Campus, for its advanced research resources and facilities and all provided supports.

REFERENCES

[1] Luque, A. and Hegedus, S. (2011) Handbook of photovoltaic science and engineering 2nd ed., Hoboken, N.J.; Chichester : John Wiley distributor.

[2] IRENA (2018) 'Solar Energy Data', [Online], Available: http://www.irena.org/solar [Accessed 23rd March 2018].

[3] Karimi, M., Mokhlis, H., Naidu, K., Uddin, S. and Bakar, A. H. A. (2016) 'Photovoltaic penetration issues and impacts in distribution network – A review', Renewable and Sustainable Energy Reviews, vol.53, pp.594-605.

[4] Kyritsis, A., Voglitsis, D., Papanikolaou, N., Tselepis, S., Christodoulou, C., Gonos, I. and Kalogirou, S. A. (2017) 'Evolution of PV systems in Greece and review of applicable solutions for higher penetration levels', Renewable Energy, vol.109, pp.487-499.

[5] Moeed Amjad, A. and Salam, Z. (2014) 'A review of soft computing methods for harmonics elimination PWM for inverters in renewable energy conversion systems', Renewable and Sustainable Energy Reviews, vol.33, pp.141-153.

[6] Martin, D., Goodwin, S., Krause, O., et al. (2014): 'The effect of PV on transformer ageing: University of Queensland's experience'. Australasian Universities Power Engineering Conf., pp. 1–6.

[7] HUAWEI (2018) 'Smart String Inverter (SUN2000-8/12KTL)', [Online], Available: solar.huawei.com/en-eu/commercial/3.pdf [Accessed 6th Feb 2018].

[8] EU (2018) 'Photovoltaic Geographical Information System (PVGIS)', [Online], Available: http://re.jrc.ec.europa.eu/pvgis.html [Accessed 3rd Feb 2018].

[9] Erickson, R. W. (2001) Fundamentals of power electronics, 2nd ed., Boston, Mass.; Great Britain: Kluwer Academic Publishers.

[10] IEEE Recommended Practice and Requirements for Harmonic Control in Electric Power Systems," in IEEE Std 519-2014 (Revision of IEEE Std 519-1992), pp.1-29, 11 June 2014.

[11] T. M. Blooming and D. J. Carnovale, "Application of IEEE STD 519-1992 Harmonic Limits," Conference Record of 2006 Annual Pulp and Paper Industry Technical Conference, Appleton, WI, 2006, pp. 1-9.

[12] Chidurala, A., Saha, T. K. and Mithulananthan, N. (2016) 'Harmonic impact of high penetration photovoltaic system on unbalanced distribution networks – learning from an urban photovoltaic network', IET Renewable Power Generation, vol.10(4), pp.485-494.

[13] Papaioannou, I. T., Bouhouras, A. S., Marinopoulos, A. G., Alexiadis, M. C., Demoulias, C. S. and Labridis, D. P. (2008) Harmonic impact of small photovoltaic systems connected to the LV distribution network, pp. 1-6.

[14] R. O. Anurangi, A. S. Rodrigo and U. Jayatunga (2017), "Effects of high levels of harmonic penetration in distribution networks with photovoltaic inverters," 2017 IEEE International Conference on Industrial and Information Systems (ICIIS), pp. 1-6.

[15] Ayub, Munirah & Gan, Chin & Abdul Kadir, A. F. (2014). The impact of grid-connected PV systems on Harmonic Distortion. 2014 IEEE Innovative Smart Grid Technologies. pp.669-674.

[16] Dartawan, K., Austria, R., Hui, L. and Suehiro, M. (2012) 'Harmonics issues that limit solar photovoltaic generation on distribution circuit', SOLAR 2012, World Renewable Energy Forum (WREF 2012), pp.1-7.

[17] Srinath, S., Poongothai, M. S. and Aruna, T. (2017) 'PV Integrated Shunt Active Filter for Harmonic Compensation', Energy Procedia, 117, pp.1134-1144.

[18] Zammit, D., Spiteri Staines, C., Apap, M. and Licari, J. (2017) 'Design of PR current control with selective harmonic compensators using Matlab', Journal of Electrical Systems and Information Technology, vol.4(3), pp.347-358.

[19] Yang, Y., Zhou, K. and Blaabjerg, F. (2016) 'Current Harmonics From Single-Phase Grid-Connected Inverters—Examination and Suppression', IEEE Journal of Emerging and Selected Topics in Power Electronics, vol.4(1), pp.221-233.

[20] Bouloumpasis, I. D., Vovos, P. N., Georgakas, K. G. and Vovos, N. A. (2016) 'Harmonic Cancellation of PV-supplied DC/AC Converter without Stabilizing Input Capacitors', IFAC-PapersOnLine, vol.49(27), pp.35-40.

[21] M. A. A. Mohd Zainuri, M. A. Mohd Radzi, A. Che Soh, N. Mariun, N. Abd Rahim, J. Teh, C. M. Lai. (2018). 'Photovoltaic Integrated Shunt Active Power Filter with Simpler ADALINE Algorithm for Current Harmonic Extraction'. Energies, vol.11(5), p.1152.

[22] Z. B. Esmaeil, S. S. Mohammad, E. Esmaeil, B. Frede. (2018). 'Adaptive-Harmonic Compensation in Residential Distribution Grid by Roof-Top PV Systems'. IEEE Journal of Emerging and Selected Topics in Power Electronics. vol.6(4), pp.2098-2108.

[23] A. Latheef, D. A. Robinson, Gosbell, V. J. and Smith, V. W. (2006) 'Harmonic impact of photovoltaic inverters on low voltage distribution systems', in Conference Proceedings of the 2006 Australasian Universities Power Engineering Conference, pp. 1-6.

[24] MathWorks (2018) '250-kW Grid-Connected PV Array', [Online], Available: goo.gl/2PjqZh [Accessed 1st July 2018].

[25] Bhardwaj, M. and Subharmanya, B. (2013) 'PV Inverter Design Using Solar Explorer Kit', Texas Instruments Incorporated, pp.19-20.

[26] de Brito, Moacyr & Sampaio, Leonardo & Luigi, G & Melo, Guilherme & Canesin, C.A.. (2011). 'Comparative analysis of MPPT techniques for PV applications'. 3rd International Conference on Clean Electrical Power: Renewable Energy Resources Impact, pp. 99-104.

[27] Chidurala, A., Saha, T. K. and Mithulananthan, N. (2016) 'Harmonic impact of high penetration photovoltaic system on unbalanced distribution networks – learning from an urban photovoltaic network', IET Renewable Power Generation, vol.10(4), pp.485-494.

[28] NREL(2013), 'PSCAD Modules Representing PV Generator', [Online]. Available: http://www.nrel.gov/docs/fy13osti/58189.pdf. [Accessed 4th July 2018].

[29] Kalair, A., Abas, N., Kalair, A. R., Saleem, Z. and Khan, N. (2017) 'Review of harmonic analysis, modeling and mitigation techniques', Renewable and Sustainable Energy Reviews, vol.78, pp.1152-1187.

[30] MTECorp (2012) 'RL Line Load Reactors', [Online], Available: https://goo.gl/b5itHd [Accessed 1st July 2018].

[31] Deng, Zhida, Rotaru, Mihai and Sykulski, Jan (2017) Harmonic Analysis of LV distribution networks with high PV penetration. In 2017 International Conference on Modern Power System, pp.1-6.

[32] Rangarajan, S. S., Collins, E. R. and Fox, J. C. (2017) 'Comparative impact assessment of filter elements associated with PWM and hysteresis-controlled PV on network harmonic resonance in distribution systems', 2017 IEEE 6th International Conference on Renewable Energy Research and Applications, pp. 80-85.

Lue Xiong received his BEng with First Class Honors in Electrical and Electronic Engineering and MSc with Distinction in Renewable Energy from University of Strathclyde and Heriot-Watt University Dubai in 2013 and 2018 respectively. His research interests lie in the impact of renewable generation on power system stability and relevant smart grid technologies.

Dr Mutasim Nour is currently working in Heriot-Watt University, School of Engineering and Physical Sciences, and holds the position Director of MSc Energy and Renewable Energy programs in Dubai Campus. Prior to joining Heriot-Watt University, Dr. Nour was an Associate Professor at the University of Nottingham Malaysia Campus. Dr. Nour research interest includes renewable energy and demand management, Energy efficiency, power electronics, and fuzzy logic control. He is currently involved in several research activities which include: PV inverter system and PV solar tracker. Energy demand management, Renewable Energy Storage Systems and Applications of Artificial Intelligence to Power Systems.

Dr. Eyad Radwan started his academic career in 1999 when he joined UCSI University (Malaysia) as lecturer in the Electrical Engineering Department. In 2005, Dr. Radwan became an Associate Professor and worked as Head for the School of Engineering. From 2007-to- 2009 he was appointed as the Dean of the Faculty of Engineering, Architecture & Built Environment at UCSI University. Since 2012, Dr. Radwan has been working with the Applied Science University in Amman Jordan. He holds the rank of Associate Professor and teaches courses in the area of Electrical Machines, Automatic Control, and Electrical Drives.